Irregular Grain Structure in Micromagnetic Simulation

D. G. Porter, E. Glavinas, P. Dhagat, J. A. O'Sullivan, R. S. Indeck and M. W. Muller
Magnetics and Information Science Center, Department of Electrical Engineering,
Washington University, St. Louis, MO USA 63130-4899

Abstract— **A randomized microstructure based on the Voronoi diagram is proposed for micromagnetic models. Simulations illustrate variability of extrinsic magnetic properties with microstructure, medium noise dependence on medium properties, and jitter dependence on trackwidth.**

I. Introduction

Much research into the structural details of the magnetic patterns which store information in magnetic recording systems has been based on micromagnetic models of magnetic recording media [1], [2], [3], [4]. Most of these models make use of a regular grain structure, tiling the medium plane with a spatially periodic array of hexagons or rectangles. Regular grain structures have a number of advantages, including the property that they form a space-filling partition of the medium plane. However, Miles has demonstrated that such microstructure regularity yields unphysical anisotropic properties [5], and has proposed an alternative randomized grain geometry [6], [7]. In the alternative strategy, grains are placed at random in the medium plane with care taken not to allow grain overlap. This strategy generates isotropic microstructures, but a multistage process is necessary to achieve an acceptable packing fraction.

In this manuscript we present a micromagnetic model with randomized microstructure as a generalization of regular microstructure models. The resulting grain geometry is irregular, and also forms a partition of the medium plane with no gaps between grains. The grain generation algorithm is built on the concept of the Voronoi diagram [8].

II. Irregular Grain Geometry

Let $S \subset \mathbf{R}^2$ be a set of N planar points, $\{P_1, \ldots, P_N\}$. The *Voronoi diagram* of S, $\mathcal{V}(S)$, is the set of regions $\{R_1, \ldots, R_N\}$, where

$$R_k = \{x \in \mathbf{R}^2 : \forall_{l \neq k} : \|x - P_k\| \leq \|x - P_l\|\} \qquad (1)$$

The computation of the Voronoi diagram is a well-studied problem in the field of computational geometry and can be performed using software available from The Geometry Center at the University of Minnesota [9]. When the set of initial points S is a lattice, the Voronoi diagram has a regular structure. Figure 1 illustrates the generation of a hexagonal grain structure as the Voronoi diagram of a lattice S. A generalization to irregular structures is achieved by choosing a randomly dispersed set of initial points S. Figure 2 illustrates the generation of an irregular grain structure as the Voronoi diagram of a set of points S generated by a Poisson point process [10] .

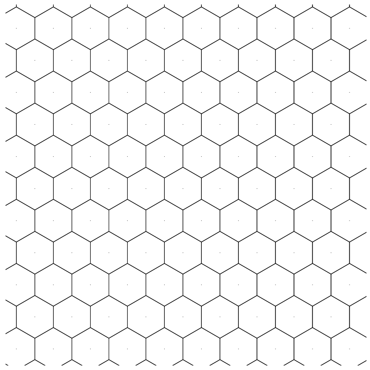

Fig. 1. Hexagonal grain structure

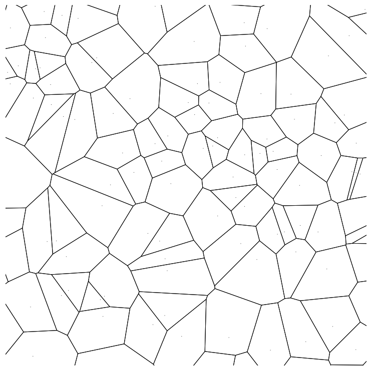

Fig. 2. Irregular grain structure

Because the Voronoi diagram is a partition of the medium plane, this method of generating randomized microstructure does not encounter the difficulty of a low packing fraction. In addition, Voronoi regions are an attractive grain model because they approximate the structure which results from crystal growth outward from nucleation sites represented by the points in S.

Three magnetic interactions are represented. Each grain exhibits uniaxial anisotropy with an easy axis chosen at random. The magnetic interactions are represented by dipole-dipole interactions computed at the centroids of the grains with moments proportional to grain area. This simple representation is accurate for long-range interactions. Short range magnetostatic interactions are expected to be dominated by exchange interactions. Exchange interactions are computed in such a way as to split the exchange energy of a domain wall equally between each pair of grains which share an edge, following Muller and Indeck [11]. Therefore, the exchange interaction between two grains is proportional to the length of the edge they share. Grains

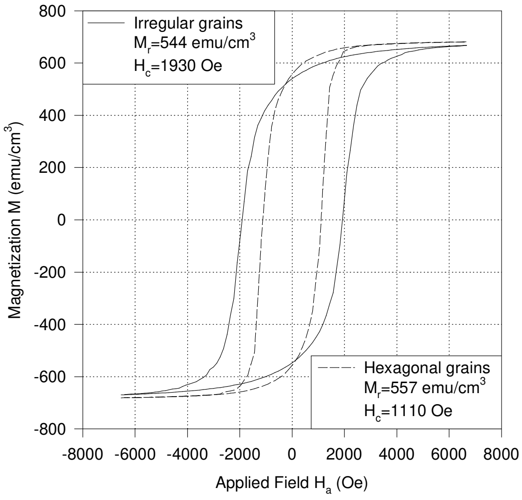

Fig. 3. Hysteresis loops for hexagonal and irregular grain structures

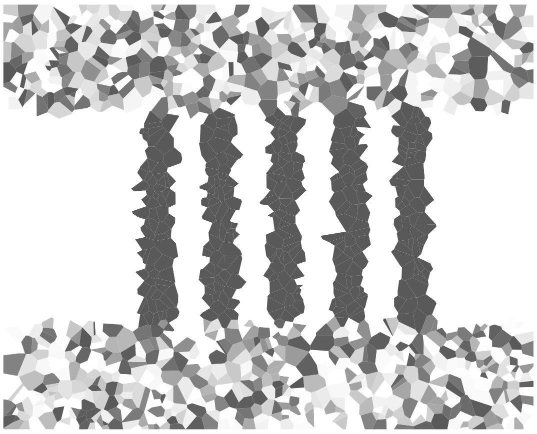

Fig. 4. High-density data pattern

are selected in a random sequence. The magnetization of each selected grain is rotated in the medium plane in response to its local field until it reaches a local minimum of magnetic energy. It has been demonstrated that the final magnetization state of this evolution algorithm is nearly sure to be a local minimum of total magnetic energy [12].

III. Simulation Results

To compute hysteresis loops, two 2μm $\times$ 2μm medium patches were generated, one of hexagonal grains, the other of irregular grains. The grains were generated to have an average area of 2500 nm^2. Each patch was initialized to a state of negative saturation. Applied field values were stepped from -1.5 to 1.5 times the anisotropy field and back in steps of 0.03 times the anisotropy field, with a complete relaxation to a stable state at each step of the computation. The exact loop computed depends on the particular set of random easy axes selected. For each of the medium patches, Figure 3 contains a plot of the average of five computed hysteresis loops, where each computed loop is based on a different random selection of easy axes. The values of remanence vary by as much as 3% from the average.

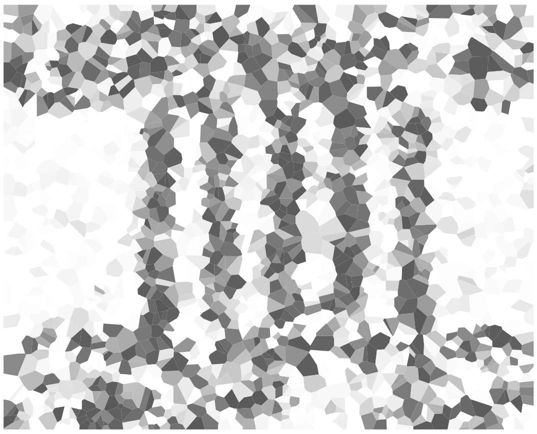

Fig. 5. Data pattern after relaxation for medium A. $M_r \cdot \delta = 1.59$ memu/cm^2. $H_c = 6800$ Oe.

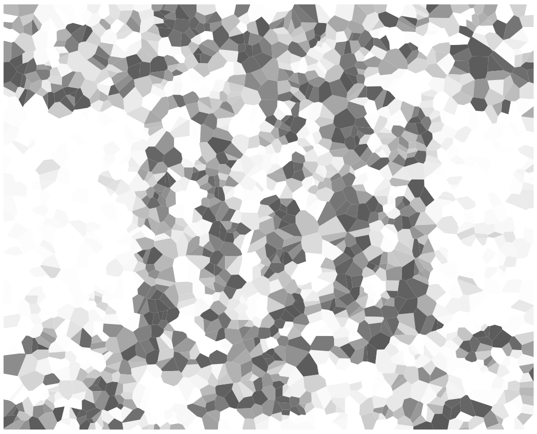

Fig. 6. Data pattern after relaxation for medium B. $M_r \cdot \delta = 1.61$ memu/cm^2. $H_c = 3100$ Oe.

Coercivity values vary as much as 11%. Significant differences in the extrinsic magnetic properties, particularly in the coercivity, arise from the different microstructures.

Figure 4 depicts a track of recorded information as represented by the model. The trackwidth is 1μm, and the bit cell length is 150 nm, values sufficient to achieve an areal density of more than 4 Gbits per square inch. The thickness of the medium, δ, is 30 nm. The initial data pattern was directly set in the simulation; it was not generated by simulation of a recording process. The grey scale of the figure represents the component of magnetization parallel to the recorded track, with white representing magnetization fully saturated toward the left and black representing magnetization fully saturated toward the right.

The magnetic pattern which remains after the interacting grains have relaxed to a stable state depends on the medium properties. Figure 5 is the pattern after relaxation for medium A with properties selected to show very little corruption of the recorded pattern. Hysteresis loop computation for medium A yields a coercivity of 6800 Oe and a remanence of 531 emu/cm^3. Figure 6 is the pattern after relaxation for medium B with somewhat more realistic properties. Hysteresis loop computation for medium B yields a coercivity of 3100 Oe and a remanence of 535

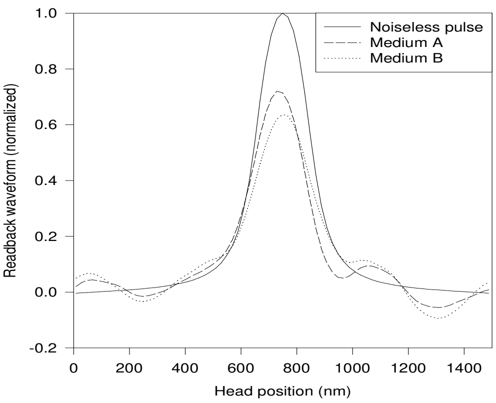

Fig. 7. Medium noise examples.

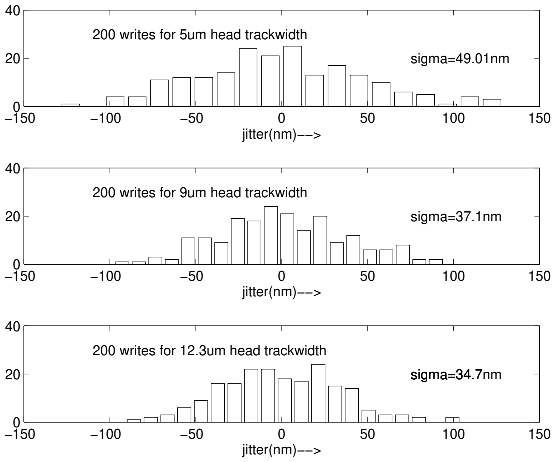

Fig. 8. Jitter histograms

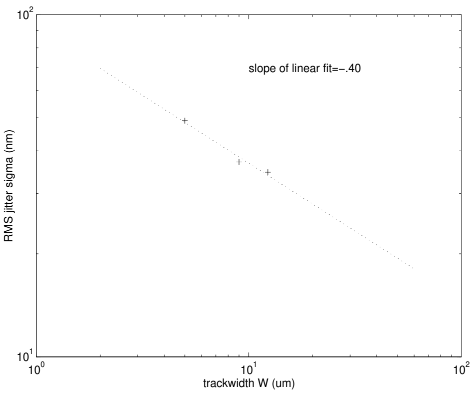

Fig. 9. Root mean square of jitter versus trackwidth

emu/cm^3. The initial "recording" can easily be recovered visually from the corrupted magnetization of medium B by viewing Figure 6 at a glancing angle from the bottom. Such a perspective approximates the integration across the trackwidth performed by a read head.

When corrupted magnetic patterns are read, the deviations of the resulting waveform from ideal are called medium noise. The read process was simulated using the Karlqvist model for an inductive read head. Figure 7 illustrates medium noise for an isolated transition recorded on both medium A and medium B, compared with the ideal pulse corresponding to an uncorrupted pattern.

One type of distortion caused by medium noise is the displacement of pulses from their intended locations [13]. This jitter has been theoretically and experimentally shown to depend on the trackwidth of the read head [14], [15]. For a trackwidth of W, the root mean square value of the jitter, σ, is predicted by theory to be

$$\sigma = CW^{-1/2}, \tag{2}$$

where C is a constant depending in part on the transverse coherence length and average grain size of the recording medium.

Simulations were performed to reproduce a set of experiments on a precision recording tester [15]. To simulate writing at many locations on a medium, 200 7.3μm $\times$ 14μm medium patches were generated with average grain area of $40,000$ nm^2 and a thickness of 50 nm. Model parameters were selected to yield a coercivity of 1250 Oe and a remanence-thickness product of 4 memu/cm^2, matching the values of the medium in the experiments. The readback pulse waveforms from isolated transitions were computed for each patch for read heads and recorded tracks of width 5, 9, and 12.3μm. The jitter values from these computed waveforms form the histograms of Figure 8. As predicted by theory, a larger trackwidth yields a smaller value of root mean square jitter. Figure 9 is a log-log plot of σ versus W, with a slope of -0.40. The simulations were also performed without allowing the interacting grains to relax to a stable state. A corresponding slope of -0.63 was computed. Neither set of simulations closely matches the theoretically predicted value of $-1/2$. However, they are qualitatively consistent with it.

IV. Acknowledgment

This work is supported in part by NSF Grants NCR-94-06197 and ECS-94-06198.

References

[1] G. F. Hughes, J. Appl. Phys. **54**, 5306 (1983).
[2] J.-G. Zhu and H. N. Bertram, J. Appl. Phys. **63**, 3248 (1988).
[3] M. Mansuripur and R. Giles, Comput. Phys. **4**, 291 (1990).
[4] J. J. Miles and B. K. Middleton, Journal of Magnetism and Magnetic Materials **95**, 99 (1991).
[5] J. J. Miles and B. K. Middleton, IEEE Trans. Magn. **26**, 2137 (1990).
[6] J. J. Miles, Ph.D. thesis, University of Manchester, 1990.
[7] J. J. Miles, M. Wdowin, J. Oakley, and B. K. Middleton, IEEE Trans. Magn. **31**, 1013 (1995).
[8] F. Aurenhammer, ACM Computing Surveys **23**, 345 (1991).
[9] C. B. Barber, D. P. Dobkin, and H. Huhdanpaa, submitted to the ACM Trans. on Mathematical Software (unpublished).
[10] D. L. Snyder and M. I. Miller, *Random Point Processes in Time and Space* (Springer-Verlag, New York, 1991).
[11] M. W. Muller and R. S. Indeck, J. Appl. Phys. **75**, 2289 (1994).
[12] D. G. Porter, Ph.D. thesis, Washington University, St. Louis, MO, 1996, in preparation.
[13] E. Glavinas *et al.*, IEEE Trans. Magn. **33**, 1069 (1997).
[14] J. J. Miles and B. K. Middleton, Journal of Magnetism and Magnetic Materials **120**, 375 (1993).
[15] P. Dhagat *et al.*, *40th Annual Conference on Magnetism & Magnetic Materials, Abstracts* (PUBLISHER, ADDRESS, 1995), pp. ED–05.